Dihydroartemisinin inhibits ATP6 activity, reduces energy metabolism of hepatocellular carcinoma cells, promotes apoptosis and inhibits metastasis via CANX

JIANG CHANG[1*], QINGZHUANG YANG[1*], XIANGWEI LIU[2], WANG LI[1] and LIANGHUI GAO[1]

[1]Department of Hepatobiliary and Pancreatic Surgery, The First Affiliated Hospital of Hainan Medical University, Haikou, Hainan 570102; [2]Department of Hepatobiliary Surgery, People's Hospital of Hetian Area, Hetian, Xinjiang 848000, P.R. China

Received April 9, 2024; Accepted July 1, 2024

DOI: 10.3892/ol.2024.14607

Abstract. Dihydroartemisinin (DHA) may inhibit the migration and invasion of liver cancer cells by reducing ATP synthase production (specifically ATP1A1 and ATP5H) through the calcium/calmodulin dependent protein kinase kinase 2/solute carrier family 8 member B1 signaling pathway. However, it is unclear whether DHA regulates ATP synthase activity by modulating other calcium ion signals to inhibit the energy metabolism and the transfer of hepatocellular carcinoma (HCC) cells. Using the Gene Expression Profiling Interactive Analysis database, a search for specific expression genes in liver cancer tissues was performed. Human HCC HuH-7 and Li-7 cells were used to produce CANX overexpression and small interfering RNA cell models. The study assessed changes in cell proliferation, apoptosis, migration and invasion. Reactive oxygen species production, ATP production, mitochondrial membrane potential (JC-1), NAD^+/NADH ratio and mitochondrial fluorescence were also evaluated. Western blotting was used to assess changes in CANX, ATP6V1 domain (ATP6V1F) and V0 domain (ATP6V0B) protein expression levels. The results demonstrated that CANX is highly expressed in liver cancer tissues. Furthermore, CANX regulated malignant biological behavior, mediated mitochondrial function and energy metabolism. However, these effects were inhibited by DHA, which decreased the expression of CANX, ATP6V0B and ATP6V1F. The findings of the present study underscore the central role of CANX in affecting the malignant biological behavior of liver cancer cells by regulating mitochondrial function and energy metabolism. Additionally, they indicate that DHA serves an anticancer role by inhibiting CANX expression.

Correspondence to: Dr Lianghui Gao, Department of Hepatobiliary and Pancreatic Surgery, The First Affiliated Hospital of Hainan Medical University, 31 Longhua Road, Longhua, Haikou, Hainan 570102, P.R. China
E-mail: gaolianghui123@126.com

*Contributed equally

Key words: calnexin, apoptosis, liver cancer, mediate mitochondrial function

Introduction

Identifying efficacious targets and therapies for hepatocellular carcinoma (HCC) remains a paramount focus in oncological research. The advent of novel biomarkers and targeted therapeutics has expanded the therapeutic landscape, rendering the quest for effective targets less daunting (1). The emergence of targeted drugs has revolutionized treatment strategies, ushering in an era of heightened therapeutic efficacy.

Calnexin (CANX), a pivotal molecular chaperone protein, is instrumental in facilitating accurate folding of glycoproteins within the endoplasmic reticulum (ER) environment. CANX is a highly reliable marker in serum that can differentiate between patients with lung cancer and healthy individuals, aiding in the early detection of lung cancer (2). N-acetylgalactosaminyltransferase activation has been shown to stimulate the glycosylation process of ER-resident CANX in both breast and liver cancer (3). CANX and ERp57 interact to facilitate the degradation of the extracellular matrix. Anti-CANX antibodies has demonstrated efficacy in inhibiting liver tumor growth and lung metastasis of breast and liver cancer cells (3). It has long been believed that calcium homeostatic regulatory signals contribute to the onset, progression and metastasis of cancer (4). In the context of calcium homeostasis, CANX serves a role in the regulation of apoptosis in dendritic cells (5). MicroRNA (miR)-148a-3p can function as a tumor promotor in colorectal cancer by targeting the CANX/major histocompatibility complex I axis, suggesting the crucial involvement of CANX in tumor immunological responses (6). CANX serves as a quality control factor for protein folding in the ER. It promotes antitumor immunotherapy and regulates several processes, including cancer cell adhesion, migration, proliferation and energy metabolism (7).

Vacuolar (V)-ATPase, a component of the energy metabolism system, influences tumor invasion and migration. V-ATPase is comprised of two components, the transmembrane V0 part and the cytoplasmic V1 part (8). ATP6V1F, a protein belonging to the ATP6V1 domain protein, constitutes

a part of the V-type ATPase complex. Central to protein folding mechanisms, it is instrumental in in upholding cellular homeostasis and ensuring environmental stability within cells (9). Overexpression of ATP6V1F in HCC tissues can accelerate the development of HCC, suppress apoptosis, encourage the migration and invasion of HCC cells, and is strongly associated with a poor prognosis for patients (10). Furthermore, bioinformatics has revealed a notable upregulation of ATP6V0B in renal cell carcinoma (11). However, the interaction between CANX and the ATP6V1 domain and V0 domain proteins is still unclear.

Dihydroartemisinin (DHA) is a derivative of artemisinin and a precursor to other active components of artemisinin. Research has reported that DHA can suppress tumor cell proliferation, induce apoptosis, reverse drug resistance and influence tumor invasion and metastasis. Additionally, DHA has an anticancer effect on lung, colorectal, pancreatic and breast cancers (12). A previous study has demonstrated that DHA inhibits the migration and invasion of HCC cells and mediated skeleton remodeling by reducing the production of ATP synthase (ATP1A1 and ATP5H) through the calcium/calmodulin dependent protein kinase kinase 2 (CaMKK2)/solute carrier family 8 member B1 (NCLX) signaling pathway (13). However, it is not clear whether DHA inhibits energy metabolism and transmission of HCC cells by regulating ATP synthase activity through other calcium ion signals. The present study aimed to elucidate the role of CANX in the progression of HCC cells and the mechanism of DHA inhibition of energy metabolism and transfer of HCC cells by regulating mitochondrial function through CANX.

Materials and methods

Cell culture. Human HCC HuH-7 and Li-7 cell lines were purchased from Shanghai Zhongqiao Xinzhou Biotechnology Co., Ltd. (https: //www.zqxzbio.com). After cell resuscitation, the cells were inoculated in RPMI-1640 medium (cat. no. C11875500BT; Thermo Fisher Scientific, Inc.) containing 10% FBS (cat. no. G24-70500; Genial Biologicals Inc) and 1% double antibody (cat. no. P1400; Beijing Solarbio Science & Technology Co., Ltd.), and cultured in a cell incubator at 37˚C in 95% air and 5% CO_2. Culture medium was replaced every 2-3 days.

Bioinformatics analysis. The Gene Expression Profiling Interactive Analysis (GEPIA) database is an online analytical tool (http://gepia.cancer-pku.cn/index.html). Based on The Cancer Genome Atlas (TCGA) and Genotype-Tissue Expression (GTEx) data, the expression difference of CANX liver cancer samples (n=369) and normal samples (n=160) was further validated through the 'expression on box plots module' of GEPIA. $P<0.05$ was considered to indicate a statistically significant difference.

cBioPortal (https://www.cbioportal.org/) is an online analytical tool and platform designed to analyze cancer genomics data from TCGA database, offering a user-friendly interface to explore complex molecular data. In the present study, CANX mutation and survival of patients analyses for CANX across liver cancer were conducted using cBioPortal.

Small interfering (si)RNA transfection and overexpression. Reagents were purchased from Sangon Biotech Co., Ltd. (https://www.sangon.com). The following sequences were constructed: CANX siRNA1, sense: 5'-ACUGGUGCUUGG AACUGCUAUUGUU-3' and antisense: 5'- AACAAUAGC AGUUCCAAGCACCAGU-3'; CANX siRNA2, sense: 5'-CGA UGAUGAAAUUGCCAAAUATT-3' and antisense: 5'-UAU UUGGCAAUUUCAUCAUCGTT-3'; and negative control (NC), sense: 5'-UUCUCCGAACGUGUCACGUTT-3' and antisense: 5'-ACGUGACACGUUCGGAATT-3'. A scrambled/non-targeting sequence acted as the negative control. Full-length CANX (Sangon Biotech Co., Ltd.) was cloned into the pcDNA3.1(+) ZB02427 vector (cat. no. 240224HY4752-2; Sangon Biotech Co., Ltd.). The empty vector was the control. HuH-7 and Li-7 cells in logarithmic growth phase were seeded in 6-well plates with $1x10^5$ cells per well. The cells were divided into control, siRNA-NC, siRNA1 and siRNA2 groups, and control, pcDNA3.1 and pcDNA3.1-NC groups. When cell fusion reached 70-80%, 100 pmol siRNA and 2.5 μg CANX overexpression plasmids were transfected at 37˚C for 24h according to the Lipo8000™ Transfection Reagent (cat. no. C0533; Beyotime Institute of Biotechnology) instructions. The transfection effects of CANX siRNA and CANX overexpression plasmids were detected by western blot analysis, as described below. Subsequent experiments were performed 24 h after transfection.

Wound-healing assay. Using a marker pen, two horizontal lines spaced 1 cm apart were drawn on the back of the 6-well plate. A total of ~$5x10^5$ Huh-7 and Li-7 cells were added into the hole. Following a 24-h incubation at 37˚C, a 200 μl pipette tip was used to scratch the cells and cross the line vertically, and the cells were washed with PBS three times. Serum-free medium was replenished for an additional 24-h culture at 37˚C. The cells were observed and imaged using a light microscope (magnification, x40; Olympus Corporation). The migratory rate of the cells was calculated from the images using Image-Pro Plus software (version 6.0; Media Cybernetics, Inc.).

Transwell cell invasion assay. At 4˚C, Matrigel (Corning, Inc.) was diluted with PBS buffer, and 100 μl was evenly precoated at 37˚C on the polycarbonate membrane surface of the upper chamber for 2 h. HuH-7 and Li-7 cells ($2x10^5$) were seeded in the upper chambers with serum-free medium. A total of 500 μl medium containing 10% FBS with or without DHA was added in the lower chambers. The cells were cultured in the incubator for 48 h at 37˚C. Upon completion of incubation, the cells were fixed with 4% paraformaldehyde for 30 min, stained with 0.1% crystal violet for 10 min at room temperature and washed with PBS 3 times. A total of five fields of vision were selected and counted under a light microscope (magnification, 200x; Olympus Corporation).

JC-1 mitochondrial membrane potential analysis. A total of $6x10^5$ HuH-7 and Li-7 cells were seeded in a 6-well plate. A total of 0.5 ml JC-1 staining working fluid (Mitochondrial Membrane Potential Assay Kit with JC-1; cat. no. M8650; Beijing Solarbio Science & Technology Co., Ltd.) was added, reverse mixed and incubated at 37˚C for 20 min. After incubation, the supernatant was discarded and the cells were washed with the JC-1 Buffer (1X). Finally, the cells were observed

and imaged using a fluorescence microscope (Olympus Corporation). The CCCP (10 mM) provided in the kit was added to the cell culture medium at a ratio of 1:1,000 and diluted to 10 μM, and was incubated with cells for 20 min. CCCP was the positive control group. Image-Pro Plus software (version 6.0; Media Cybernetics, Inc.) was used to analyze the data.

Mitochondrial fluorescence probe. HuH-7 and Li-7 cells ($1x10^5$) were incubated with Mito-Tracker Red CMXRos working solution (cat. no. C1049B; Beyotime Institute of Biotechnology) at 37˚C for 30 min. Subsequently, the Mito-Tracker Red CMXRos working solution was removed, and fresh cell culture solution pre-warmed at 37˚C was added. Finally, the cells were observed and imaged using a fluorescence microscope (Olympus Corporation). The average fluorescence density was calculated using Image-Pro Plus software (version 6.0, Media Cybernetics, Inc.).

Western blotting. HuH-7 and Li-7 cells were harvested and lysed with RIPA lysis buffer (Nanjing KeyGen Biotech Co., Ltd.) on ice. Protein concentration was determined using the BCA Protein Assay Kit (cat. no. PT0001; Leagene; Beijing Regen Biotechnology Co., Ltd.). A total of 40 μg total protein was electrophoresed using 10-12% SDS-PAGE. The separated proteins were transferred onto a PVDF membrane and the membranes were blocked with 5% skim milk powder for 1 h at room temperature. Subsequently, primary antibodies were added and incubated at 4˚C overnight. The primary antibodies used were CANX (1:5,000; cat. no. 66903-1-Ig; Proteintech Group, Inc.), ATP6V0B (1:1,000; cat. no. 27671-1-AP; Proteintech Group, Inc.) and ATP6V1F (1:1,000; ab190789; Abcam), β-actin (1:2,000; cat. no. 20536-1-AP; Proteintech Group, Inc.). The film was then washed three times with TBST (0.05% Tween 20), and then incubated with goat anti-rabbit (1:5,000; cat. no. ZB-2301; OriGene Technologies, Inc.) or anti-mouse IgG (1:5,000; cat. no. ZB-2305; OriGene Technologies, Inc.) labeled with horseradish peroxidase at room temperature for 1h. The film was washed three times with TBST again, and ECL Hypersensitive Luminescent Solution (cat. no. P1050; Applygen Technologies, Inc.) was added. The film was then transferred to the Amersham Imager 600 Automatic Chemilescence Gel Imaging Analyzer (GE Healthcare) for automatic exposure analysis. The gray values of proteins were analyzed by ImageJ software (version 1.8.0; National Institutes of Health).

ATP production. ATP content was detected using an ATP fluorescence probe (pCMV-AT1.03; cat. no. D2604; Beyotime Institute of Biotechnology). According to the user manual, the treated HuH-7 and Li-7 cells ($3x10^5$) were seeded in 12-well plates, incubated with 1 μg ATP fluorescence probe and Lipo8000™ (cat.no. C0533; Beyotime Institute of Biotechnology) for 24 h at 37˚C, and then observed and imaged using a fluorescence microscope (Olympus Corporation). Images were analyzed using Image-Pro Plus software (version 6.0; Media Cybernetics, Inc.).

NAD^+/NADH. The HuH-7 and Li-7 cells ($1x10^5$) were inoculated on 6-well plates. After the transfection and drug treatment in each group, the culture medium was discarded and washed with PBS. After washing, 1 ml of NAD^+/NADH extraction solution (cat. no. S0175; Beyotime Institute of Biotechnology) was added to each well, and the supernatant was obtained after centrifugation. A 100 μl sample to be tested was transferred to the centrifuge tube and heated at 60˚C for 30 min to decompose NAD^+. Subsequently, the 20 μl supernatant was added into a 96-well plate. The samples were incubated with 90 μl alcohol dehydrogenase working solution at 37˚C for 10 min for measuring the NADH content. They were then incubated with 10 μl color developing solution at 37˚C for 10 min. After mixing, the absorbance at 450 nm was measured and the of NAD^+/NADH content was calculated according to the standard curve.

Cell Counting Kit-8 (CCK-8) assay. HuH-7 and Li-7 cells ($2x10^3$) were seed in 96-well plates and then 10 μl CCK-8 reagent (cat. no. CK04; Dojindo Laboratories, Inc.) was added to each well. After a 2-h incubation, the absorbance at 450 nm was measured using a microplate reader.

TUNEL assay. According to the manufacturer's instructions (cat. no. C1090; Beyotime Institute of Biotechnology), cells were washed with PBS then fixed with 4% paraformaldehyde for 30 min at room temperature, following by PBS washing. Subsequently, cells were incubated with 0.3% Triton X-100 for 5 min at room temperature. Subsequently, 0.3% H_2O_2 in PBS was added and incubated for 20 min at room temperature. After incubation, 50 μl TUNEL working solution was added and incubated at 37˚C for 1 h. Finally, DAPI was used to stain the nucleus at room temperature for 3 min and seal the film, and then observed and imaged using a fluorescence microscope (Olympus Corporation). 3 fields of view are randomly selected. The cell death rate was calculated as ($TUNEL^+$ cells/total cells) x100.

Reactive oxygen species (ROS) detection. A Reactive Oxygen Species Detection Kit (cat. no. S0033; Beyotime Institute of Biotechnology) was used to evaluate intracellular ROS levels using a DCFH-DA probe. DCFH-DA was diluted with serum-free culture medium at a ratio of 1:1,000 to attain a final concentration of 10 μmol/l. Each group of HuH-7 and Li-7 cells ($2.5x10^5$) were incubated with the DCFH-DA working solution at 37˚C for 20 min. Rosup served as a positive control. Following incubation, fluorescence intensity was visualized using a fluorescence microscope (Olympus Corporation), imaged and analyzed using Image-Pro Plus software (version 6.0; Media Cybernetics, Inc.).

Statistical analysis. One-way analysis of variance and the Bonferroni post hoc test were applied for three groups or multi-group analysis and statistical analyses were performed using SPSS (version 26.0; IBM Corp.); visualization was carried out using GraphPad Prism (version 5; Dotmatics). $P<0.05$ was considered to indicate a statistically significant difference.

Results

CANX is highly expressed in liver cancer and is associated with survival of patients with liver cancer. The expression of CANX in liver cancer and normal tissue adjacent samples after TCGA and GTEx project data integration was analyzed using the GEPIA database. The results revealed that CANX had a significantly higher expression in the liver cancer

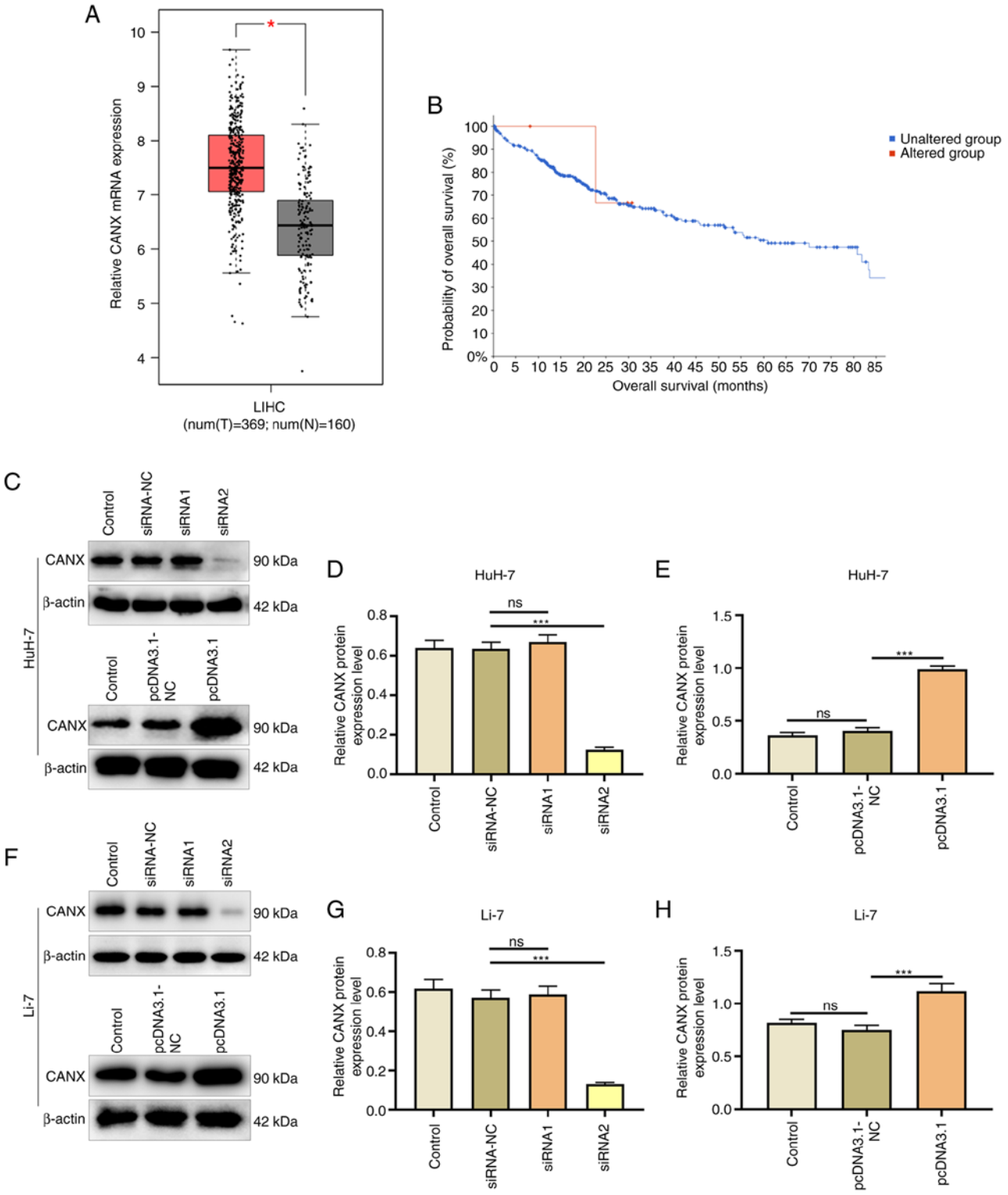

Figure 1. CANX is highly expressed in liver cancer and is associated with the survival of patients with liver cancer. (A) Box plot shows the expression of CANX in 369 liver cancer tissues and 160 normal tissues in the integrated The Cancer Genome Atlas and Genotype-Tissue Expression project data. (B) cBioPortal was used to assess the association between CANX and hepatocellular carcinoma survival. (C) Effect of CANX overexpression and siRNA in HuH-7 cells. (D) CANX siRNA efficiency in HuH-7 cells demonstrated by western blotting. (E) CANX overexpression efficiency in HuH-7 cells demonstrated by western blotting. (F) Effect of CANX overexpression and siRNA in Li-7 cells. (G) CANX siRNA efficiency in Li-7 cells demonstrated by western blotting. (H) CANX overexpression efficiency in Li-7 cells demonstrated by western blotting. The relative protein expression level was semi-quantified using Image J software. *P<0.05; ***P<0.001. ns, not significant; CANX, calnexin; T, tumor; N, normal; LIHC, liver hepatocellular carcinoma; siRNA, small interfering RNA; NC, negative control.

samples (n=369) compared with that in the normal adjacent tissue samples (n=160; Fig. 1A). In addition, cBioPortal was used to analyze the effect of CANX on patient survival, and the results demonstrated that CANX gene expression was associated with survival and CANX mutations were negatively correlated with survival (Fig. 1B). Furthermore, the effects of

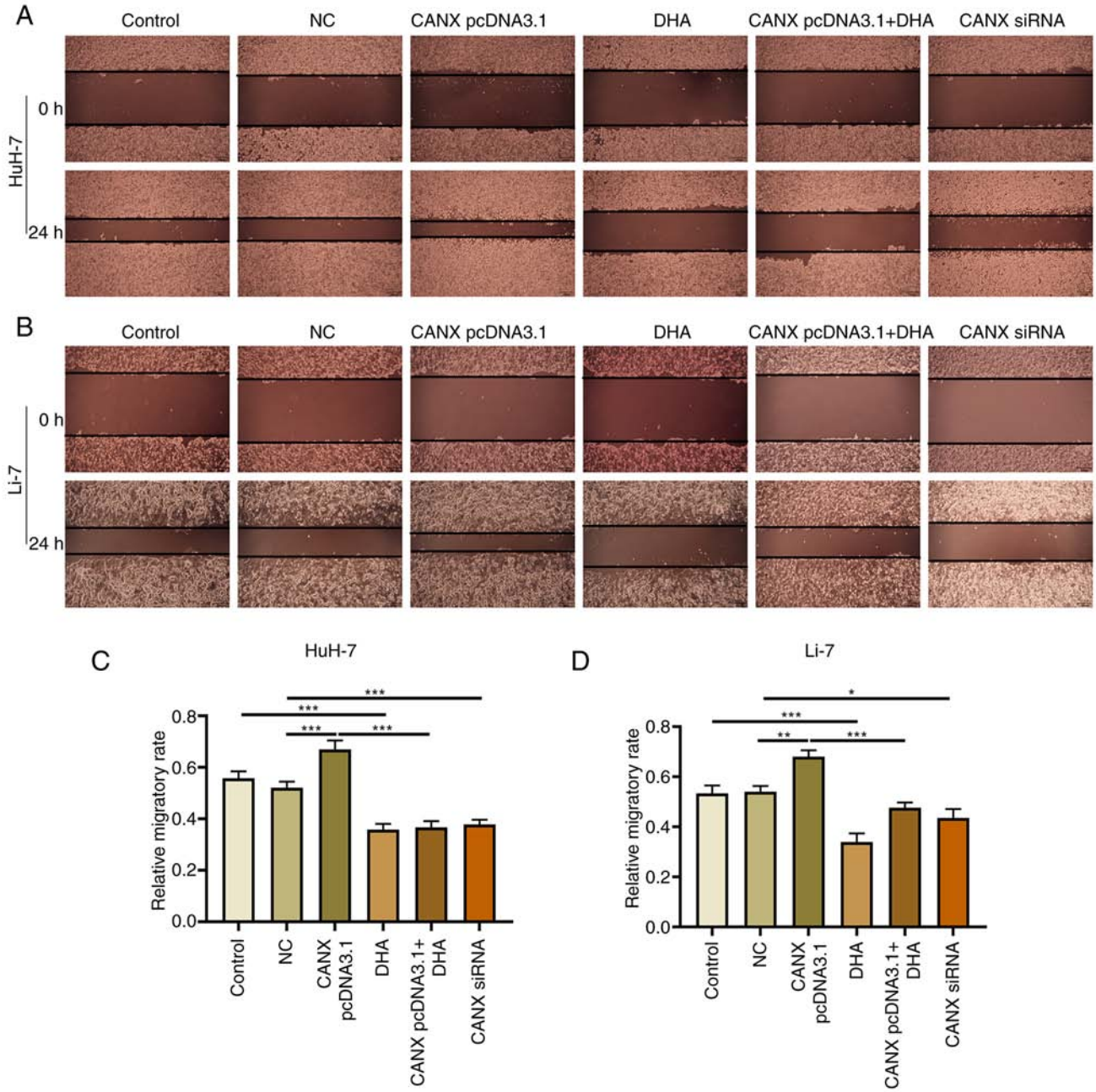

Figure 2. Effect of CANX and DHA on cell migration in HuH-7 and Li-7 cells. Representative images of (A) HuH-7 and (B) Li-7 cells with CANX knockout, DHA or CANX overexpression. Wound distance in (C) HuH-7 and (D) Li-7 cells, quantified by Image-Pro Plus 6.0 software. (scale bar, 200 μm). *P<0.05; **P<0.01; ***P<0.001. CANX, calnexin; DHA, dihydroartemisinin; NC, negative control; siRNA, small interfering RNA.

the CANX overexpression plasmid and siRNA were assessed (Fig. 1C-H). Western blotting revealed that Compared with the pcDNA3.1-NC group, the overexpression plasmid (pcDNA3.1 group) significantly increased CANX expression. Furthermore, the interference effect of CANX siRNA2 was significant compared with siRNA-NC, and therefore it was chosen for use in subsequent experiments.

Effects of CANX and DHA on invasion and migration of liver cancer cells. Cell scratch and Transwell experiments demonstrated that overexpression of CANX significantly increased the migration and invasion of liver cancer cells compared with the NC group. Moreover, the results revealed that CANX siRNA significantly inhibited the migration and invasion of liver cancer cells compared with the NC group and DHA significantly inhibited the migration and invasion of liver cancer cells compared with the control group (Figs. 2 and 3). Notably, the combination of DHA and CANX overexpression inhibited cell invasion and migration (Figs. 2 and 3). The results indicate that CANX can mediate the metastasis of liver cancer cells, and this regulatory effect can be inhibited by DHA.

Effects of CANX and DHA on proliferation and apoptosis of liver cancer cells. The results of the cell proliferation experiment demonstrated that overexpression of CANX significantly increased the proliferation rate of cells compared with the NC group, whilst knockdown of CANX (compared with

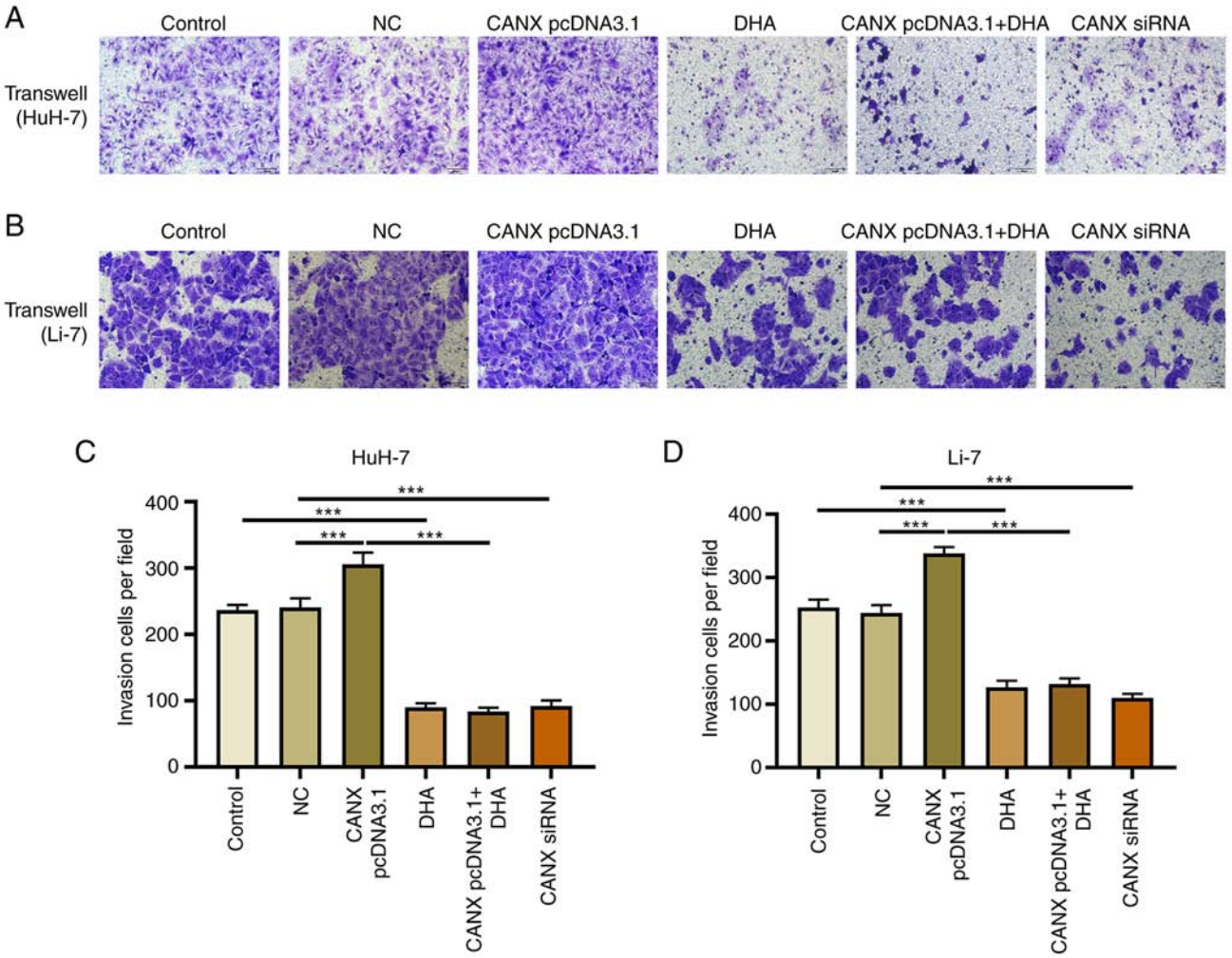

Figure 3. Effect of CANX and DHA on cell invasion in HuH-7 and Li-7 cells. Transwell assay for assessing cell invasion after CANX knockout, DHA or CANX overexpression in (A) HuH-7 and (B) Li-7 cells. The number of invasive (C) HuH-7 and (D) Li-7 cells (scale bar, 50 μm). ***P<0.001. CANX, calnexin; DHA, dihydroartemisinin; NC, negative control; siRNA, small interfering RNA.

the NC group) and DHA (compared with the control group) administration exerted a significant inhibitory effect (Fig. 4A and B). Furthermore, the combination of DHA and CANX overexpression significantly inhibited the proliferation of liver cancer cells compared with the CANX pcDNA3.1 group (Fig. 4A and B). However, apoptosis experiments revealed that there was no significant change in the apoptosis rate of overexpressed CANX cells compared with the NC group, whilst knockdown of CANX expression (compared with the NC group) and DHA (compared with the control group) significantly increased the apoptosis rate. Moreover, the combination of DHA and CANX overexpression significantly increased the apoptosis rate compared with the CANX pcDNA3.1 group (Fig. 4C-F). The aforementioned results indicate that CANX can mediate apoptosis and proliferation; however, DHA can inhibit the overexpression of CANX-mediated regulation in addition to inhibiting the proliferation and promoting apoptosis of HCC cells alone.

Effects of CANX and DHA on mitochondrial ATP production and NAD$^+$/NADH ratio. Mitochondrial ATP fluorescence probe results revealed that overexpression of CANX significantly upregulated ATP fluorescence intensity, whilst knockdown of CANX significantly decreased it, compared with the NC group (Fig. 5A-C). The change in NAD$^+$/NADH ratio was also associated with energy metabolism: Overexpression of CANX significantly increased the NAD$^+$/NADH ratio, whilst knockdown of CANX significantly reduced the NAD$^+$/NADH ratio compared with the NC group (Fig. 5D and E). Furthermore, treatment with DHA alone (compared with the control group) or in combination with CANX overexpression (compared with the CANX pcDNA3.1 group) significantly reduced ATP production and the NAD$^+$/NADH ratio in HCC cells (Fig. 5D and E). The results indicate that CANX can mediate mitochondrial ATP production and the NAD$^+$/NADH ratio, thereby it participates in the energy metabolism of HCC cells. However, the results also indicates that DHA can inhibit CANX-mediated energy production.

Effects of CANX and DHA on mitochondrial membrane potential. Mitochondria play a central role in energy metabolism (14). The mitochondrial membrane potential and Mito-Tracker Red CMXRos assays revealed that overexpression of CANX significantly upregulated the mitochondrial membrane potential level compared with the NC group,

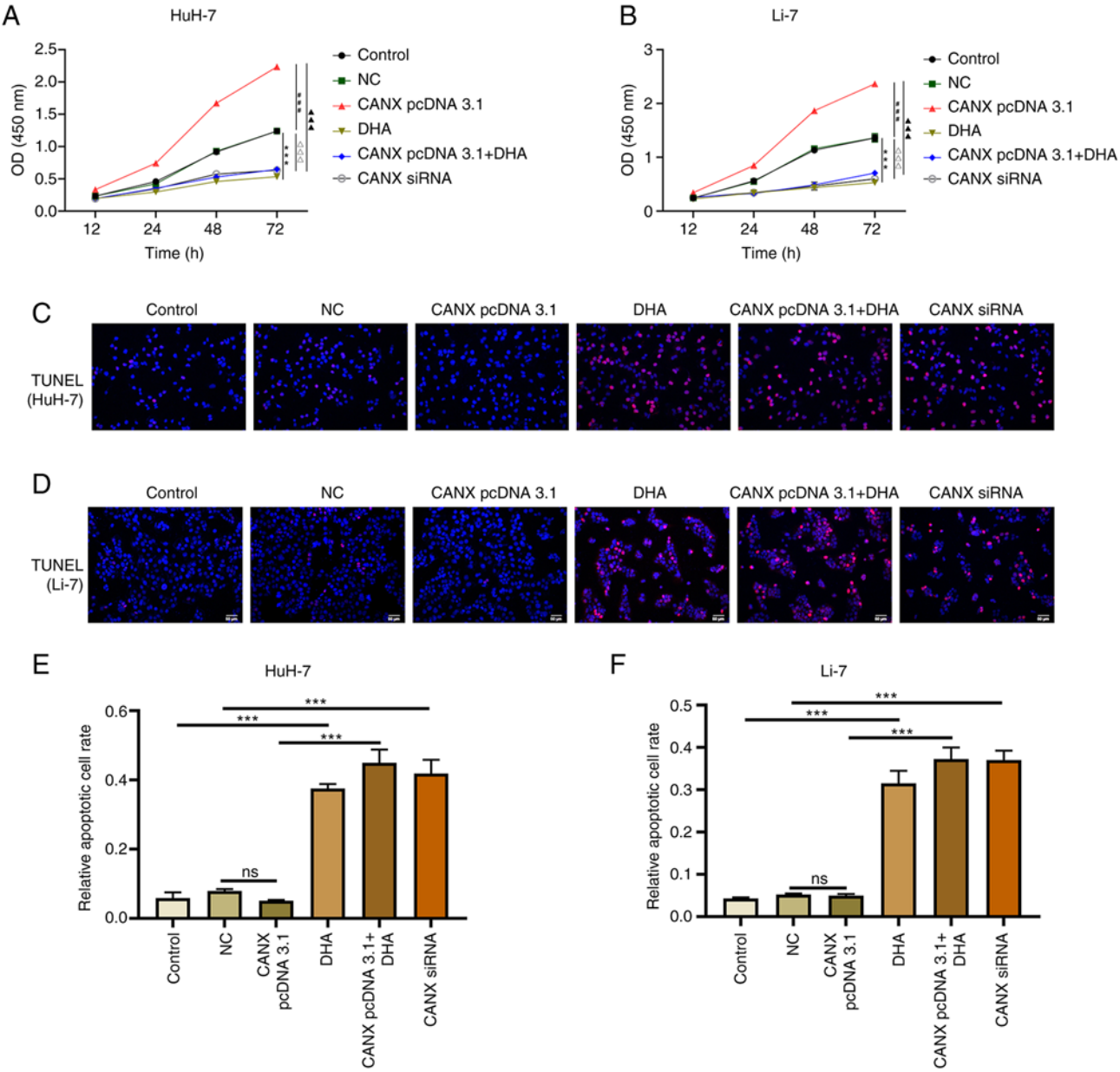

Figure 4. Effects of CANX and DHA on the proliferation and apoptosis of liver cancer cells. Cell Counting Kit-8 assays detected the cell proliferation of (A) HuH-7 and (B) Li-7 cells with CANX knockout, DHA or CANX overexpression. ***P<0.001, control vs. DHA; $^{###}$P<0.001, NC vs. CANX pcDNA3.1; ^{ΔΔΔ}P<0.001, NC vs. CANX siRNA; $^{▲▲▲}$P<0.001, CANX pcDNA3.1cCANX pcDNA 3.1+DHA. TUNEL assays assessed the rate of apoptosis of (C) Huh-7 and (D) Li-7 cells after CANX knockout, DHA or CANX overexpression. The apoptotic cell rate of (E) HuH-7 and (F) Li-7 cells (scale bar, 50 μm). ***P<0.001. CANX, calnexin; DHA, dihydroartemisinin; NC, negative control; siRNA, small interfering RNA; ns, not significant.

and aggregation or small flaky red fluorescence signals was observed. Furthermore, knockdown of CANX and DHA administration significantly reduced the fluorescence intensity of the mitochondrial membrane potential, showing a sparse scattered pattern (Fig. 6). Notably, DHA inhibited the role of CANX overexpression in mediating mitochondrial membrane potential.

Effects of CANX on ROS production in liver cancer cells. ROS serve a pivotal role in mitochondrial dysfunction and decreased energy metabolism (15,16); however, changes in ROS levels can have a direct impact on the progression of liver cancer cells (17). Overexpression of CANX significantly inhibited the production of ROS, compared with the NC group, with decreased green fluorescence intensity observed. Moreover, knockdown of CANX (compared with the NC group) and DHA (compared with the control group) administration significantly promoted ROS production, with enhanced green fluorescence intensity observed (Fig. 7). The results indicate that a combination of DHA and CANX overexpression can significantly promote ROS production in HCC cells.

Effects of CANX and DHA on ATP6V0B and ATP6V1F expression. ATP6V1 and V0 domain proteins participate in acid-base balance and membrane transport, and serve an indispensable role in the energy metabolism mechanism (18). The results of the present study demonstrated that compared

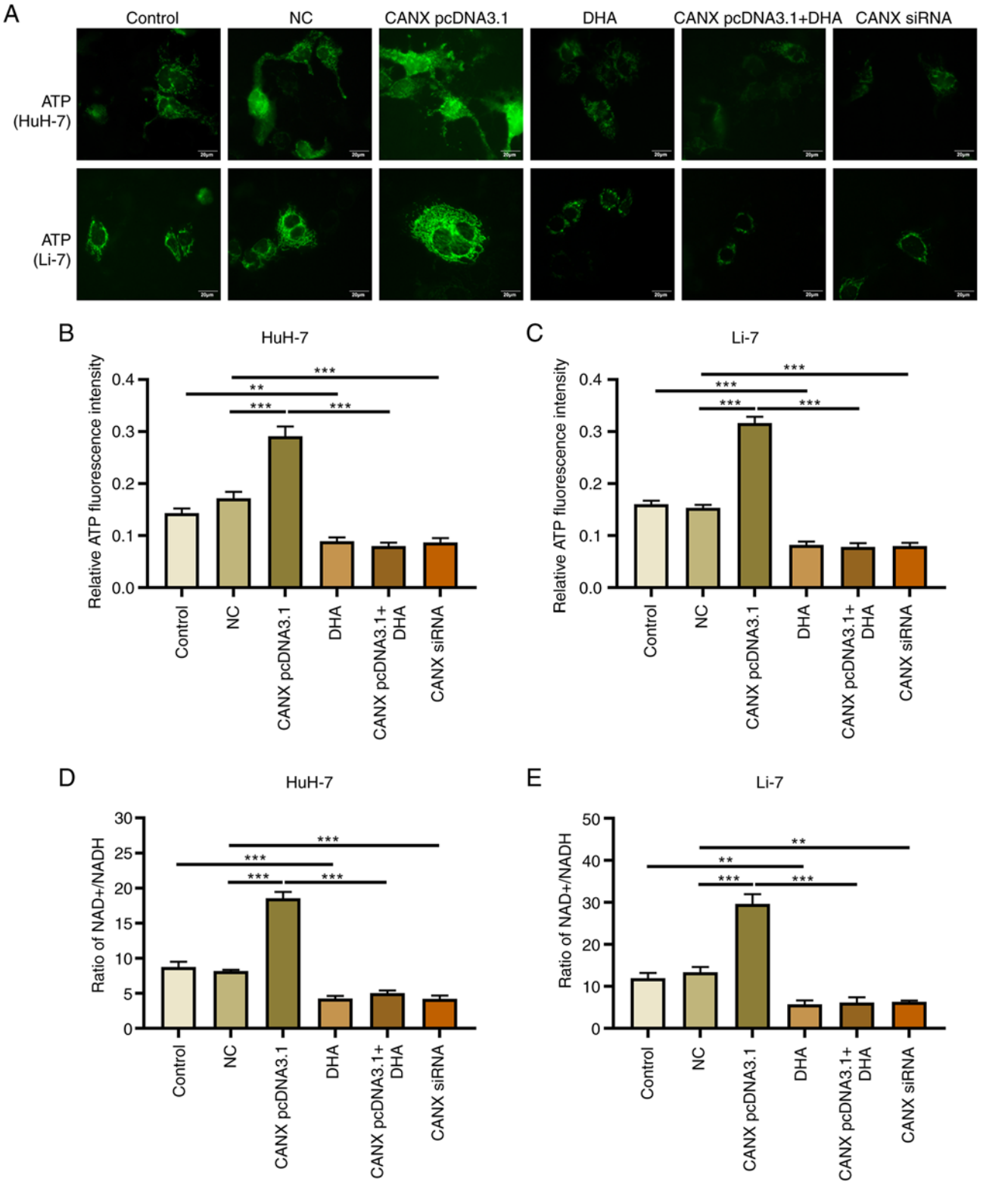

Figure 5. Effects of CANX and DHA on mitochondrial ATP production and the NAD^+/NADH ratio. (A) ATP fluorescence intensity probe detected ATP fluorescence intensity of HuH-7 and Li-7 cells after CANX knockout, DHA or CANX overexpression. Level of ATP fluorescence intensity in (B) HuH-7 and (C) Li-7 cells, quantified using Image-Pro Plus 6.0 software. Ratio of NAD^+ and NADH content in (D) HuH-7 and (E) Li-7 cells after CANX knockout, DHA or CANX overexpression (scale bar, 20 μm), **P<0.01; ***P<0.001. CANX, calnexin; DHA, dihydroartemisinin; NC, negative control; siRNA, small interfering RNA.

with the NC group, overexpression of CANX significantly promoted the expression of ATP6V0B and ATP6V1F, whereas the expression of ATP6V0B and ATP6V1F was significantly downregulated by CANX siRNA compared with the NC group. Moreover, compared with the control group, DHA administration significantly decreased the expression of CANX. In addition, compared with the CANX pcDNA3.1 group, the expression of ATP6V0B and ATP6V1F reduced when

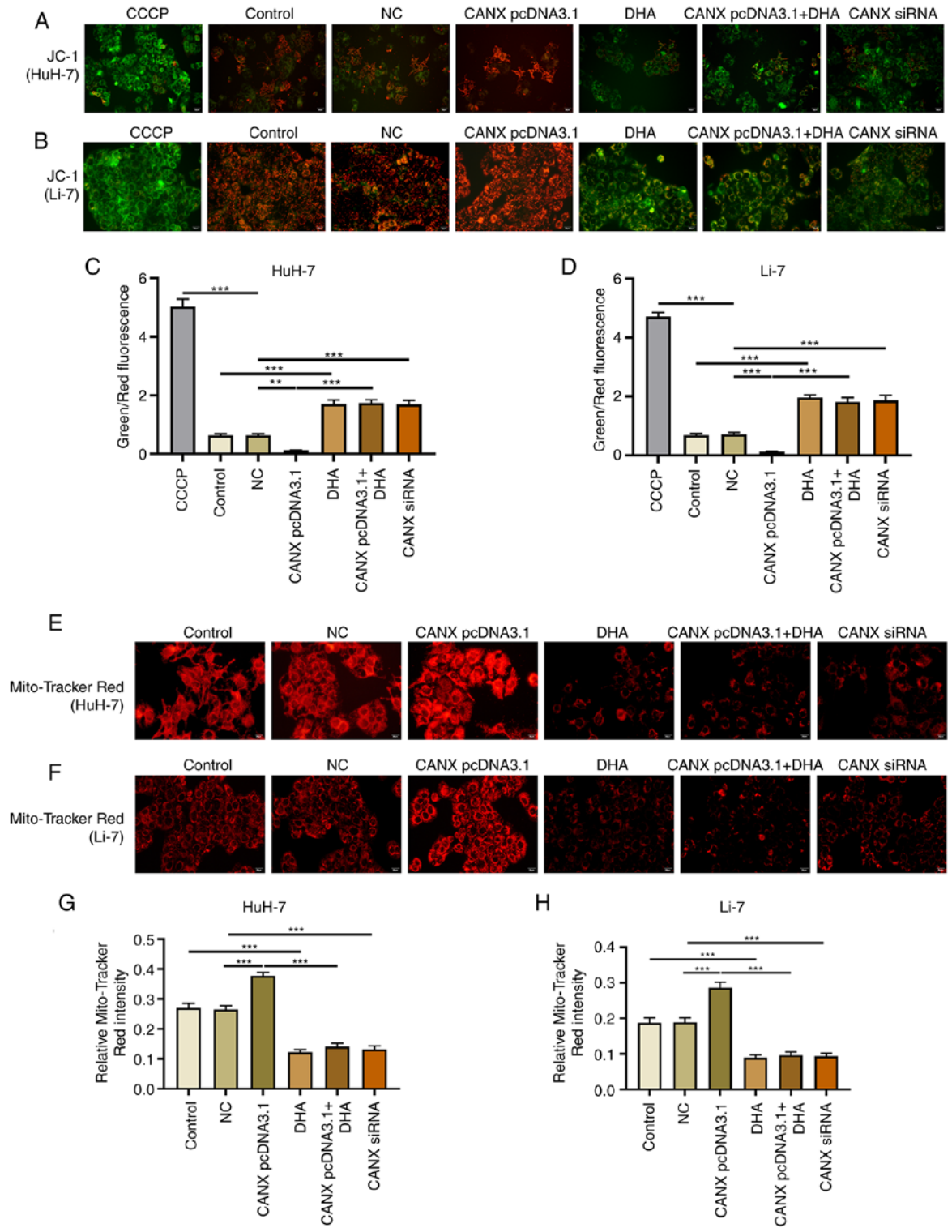

Figure 6. Effects of CANX and DHA on mitochondrial membrane potential. JC-1 assay assessed mitochondrial membrane potential levels of (A) HuH-7 and (B) Li-7 cells after CANX knockout, DHA or CANX overexpression. Level of mitochondrial membrane potential in (C) HuH-7 and (D) Li-7 cells, quantified by Image-Pro Plus 6.0 software. CCCP was used as a positive control. Mitochondrial Tracker Red was used to detect the mitochondrial fluorescence intensity levels after CANX knockout, DHA or CANX overexpression in (E) HuH-7 and (F) Li-7 cells. Level of mitochondrial fluorescence intensity in (G) HuH-7 and (H) Li-7 cells, quantified by Image-Pro Plus 6.0 software. ***P<0.001. CANX, calnexin; DHA, dihydroartemisinin; NC, negative control; siRNA, small interfering RNA; CCCP, carbonyl cyanide-m-chlorophenylhydrazone.

cells were treated with a combination of DHA and CANX overexpression (Fig. 8). These findings indicate that CANX is involved in the regulation of the molecular mechanism of energy metabolism in HCC cells, highlighting that CANX may be a viable target of DHA.

Discussion

Energy metabolism and mitochondrial function are linked to the balance maintained by the calcium homeostatic control system (19). A pivotal approach in curtailing tumor cell

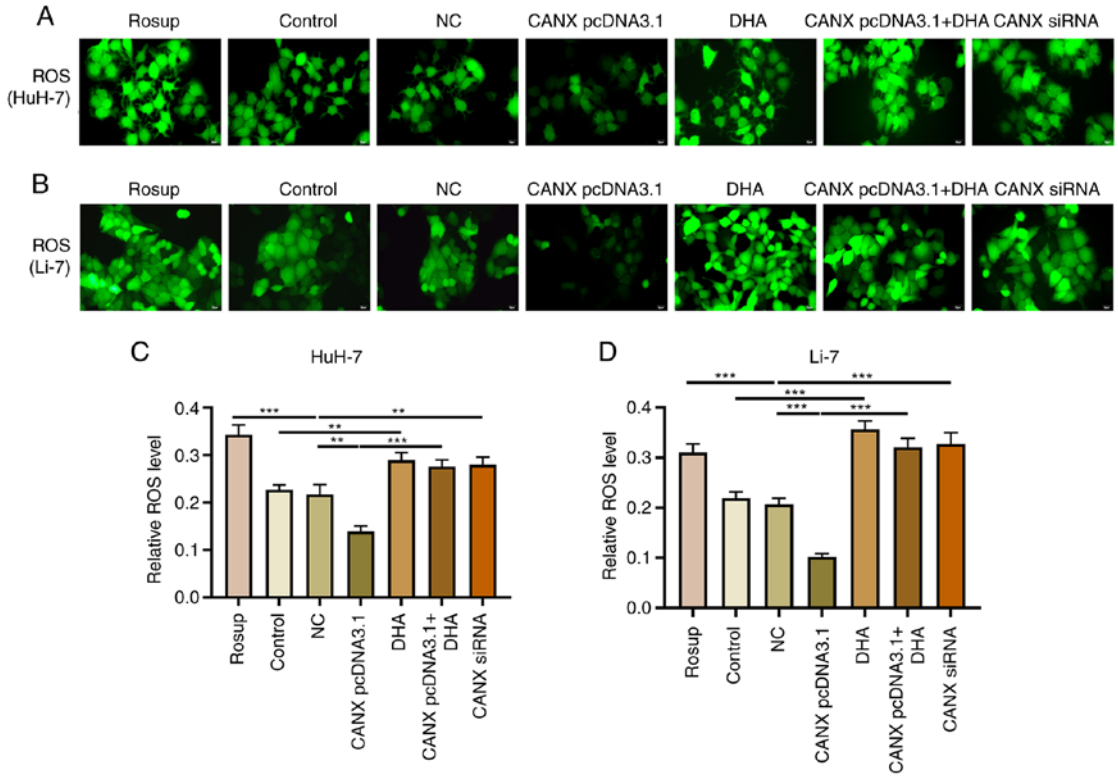

Figure 7. Effects of CANX on ROS production in liver cancer cells. ROS production was evaluated using DCFH-DA staining after CANX knockout, DHA or CANX overexpression in (A) HuH-7 and (B) Li-7 cells. Level of ROS in (C) HuH-7 and (D) Li-7 cells, quantified using Image-Pro Plus 6.0 software (scale bar, 20 μm). **P<0.01; ***P<0.001. CANX, calnexin; DHA, dihydroartemisinin; NC, negative control; siRNA, small interfering RNA; ROS, reactive oxygen species.

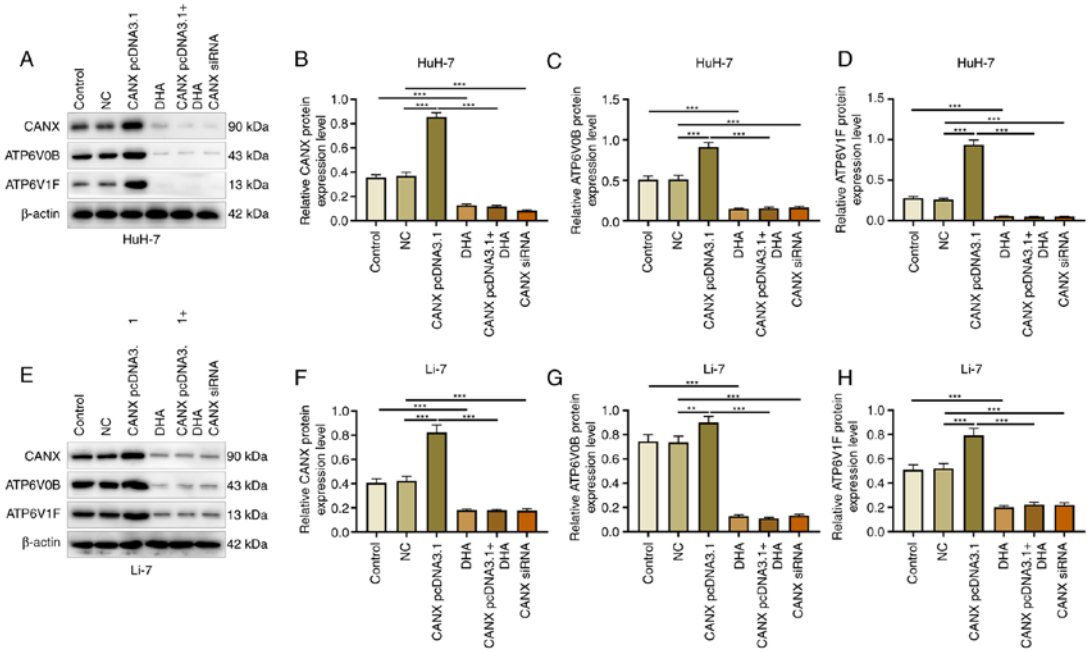

Figure 8. Effects of CANX and DHA on ATP6V0B and ATP6V1F expression. (A) Expression of (B) CANX, (C) ATP6V0B and (D) ATP6V1F in HuH-7 cells, detected by western blotting after CANX knockout, DHA or CANX overexpression. (E) Expression of (F) CANX, (G) ATP6V0B and (H) ATP6V1F in Li-7 cells, detected by western blotting after CANX knockout, DHA or CANX overexpression. **P<0.01; ***P<0.001. CANX, calnexin; DHA, dihydroartemisinin; NC, negative control; siRNA, small interfering RNA.

energy metabolism involves targeting key genes in calcium homeostasis regulation. CANX, a function-specific ER chaperone protein, is implicated in the mechanism of cancer and is pivotal in the storage and release of calcium ions in the ER (7,20). It was previously discovered that DHA prevented hepatoma cells from migrating and invading by decreasing

the synthesis of ATP synthase (ATP1A1 and ATP5H) via the CaMKK2/NCLX signaling pathway (13). Furthermore, the present study demonstrated that CANX serves a crucial role in liver cancer cell proliferation, apoptosis, migration and invasion, energy metabolism, mitochondrial function and ROS production. Knockdown of CANX significantly inhibited liver cancer cell progression and more significantly, DHA downregulated the expression of ATP6V0B and ATP6V1F, and regulated the energy metabolism and metastasis of liver cancer cells through CANX.

CANX is instrumental in binding, buffering and storing Ca^{2+}, thereby contributing to intracellular calcium storage. It performs as a molecular chaperone for proteins, regulates calcium homeostasis, enhances cell adhesion and preserves RNA stability and gene expression with precision (21). CANX serves a crucial role in quality control throughout the synthesis, maturation and transport of secreted and membrane proteins. Dysregulation in calcium ion homeostasis can trigger uncontrolled cell proliferation, ultimately leading to the formation of tumors (22). Studies have reported that CANX is extensively expressed in lung cancer tissues, and administration of anti-CANX antibodies has proven efficacious in eliciting substantial cytotoxic effects and suppressing tumor growth in subcutaneous xenograft experiments (2,23). This has validated CANX as a compelling therapeutic target. The anti-calnexin antibody can detect calnexin protein via exosomes, which can be applied to liquid biopsies (23). Moreover, prostate cancer cell survival has been reported to be directly impacted by CANX overexpression or knockdown in prostate cancer studies (24,25). Through the CANX/calreticulin cycle, the mutant p53 ectonucleoside triphosphate diphosphohydrolase 5 axis stimulates the production of integrin-α5 and integrin-β1, which in turn promotes the growth, metastasis and proliferation of tumor cells (26). Furthermore, in tumor cells, knocking down CD317 lowered Ca^{2+} levels in the ER by targeting calnexin and mediating tumor cell death (27). Furthermore, the results of the GEPIA database retrieval in the present study indicated that CANX is overexpressed in liver cancer tissue. The cell model of CANX knockdown and overexpression validates the pivotal role of CANX in regulating the proliferation and apoptosis of liver cancer cells, which is consistent with prior research (28,29). Moreover, the present study revealed that CANX knockdown effected apoptosis. The findings further imply that, in addition to its mediating function, CANX may serve as an independent regulatory factor to influence the progression of cancer cells. Significantly, DHA inhibits cell proliferation and apoptosis, and this effect persists when DHA was applied to the CANX overexpression group. This is in line with earlier findings (13) that DHA may impair the regulation of calcium homeostasis, thereby having an anticancer effect.

CANX serves a crucial role in the interaction between mitochondria and the smooth ER, and has a key role in the mechanism of ATP production. Over the past decade, CANX and BiP/78-kDa glucose-regulated protein, also referred to as BiP, have been identified as multifunctional ER chaperone proteins. These proteins can regulate ER and mitochondrial calcium ion homeostasis, which in turn affects mitochondrial function, and controls the rate of mitochondrial oxidative phosphorylation to regulate ATP input. This indicates the mechanism by which ER chaperones regulate ATP production and affect cellular energy metabolism (30,31). From the experimental results of the present study, CANX is involved in ATP production in liver cancer cells, regulating cell proliferation and apoptosis. This also indicates its critical role in liver cancer cell metastasis and suggests that CANX may serve a 'bridging role' in the pathway connecting the ER and the mitochondria. However, further investigation using cryo-electron microscopy is necessary. Previous research has also demonstrated that DHA may influence the energy metabolism of liver cancer cells by lowering ATP synthesis and influencing the formation of ROS via CaMKK2/NCLX signaling (13). We hypothesize that CANX represents a significant pathway through which DHA reduces energy metabolism in liver cancer cells.

Abnormal mitochondrial function is a crucial factor in mitochondria-mediated cell death, characterized by a decline in ATP production and heightened ROS production (32,33). Previous evidence has reported an interaction between acyl-CoA synthetase long chain family member 4 and CANX, which collectively modulates mitochondrial function and ATP production in cancer cells (34). Additionally, the present study demonstrated that CANX has a direct influence on mitochondrial function, which may contribute to the reduction of ATP production and promotion of ROS overproduction. Findings from a previous study demonstrated that DHA can induce ROS production (13), and in the present study, it was observed that CANX regulates ROS production in HCC cells. Notably, DHA can inhibit ROS production induced by the overexpression of CANX.

ATP6V1 domain and V0 domain proteins serve crucial roles in cancer cell progression mechanisms. ATP6V1F encodes a constituent of V-ATPase and is essential for maintaining cancer cell survival (35). ATP6V1 facilitates hydrogen ion transport, and its dysregulated expression has been implicated in the clinicopathological features of several malignancies, with notable associations observed in liver cancer studies (10,36). ATP6V1F accelerates the invasive and migratory capabilities of liver cancer cells whilst preventing cell death, thereby fostering the progression and aggressiveness of liver cancer (10). ATP6V1F is a critical gene in cell proliferation, and miR-194 operates as a tumor suppressor in digestive system cancers through the targeting of ATP6V1F (37). The present study demonstrated that CANX regulates the expression of ATP6V0B and ATP6V1F, and it was hypothesized that CANX might affect calcium homeostasis of hepatocellular carcinoma cells through ATP6. This is consistent with the findings of Singh *et al* (38). The intricate regulation of mitochondrial function relies on a network of ion signals that safeguard the integrity of energy metabolism processes (39). Notably, NCLX and leucine zipper and EF hand-containing transmembrane 1 are key players in this regulatory machinery (40). In light of the findings of earlier research (13), we hypothesize that NCLX is the likely node where DHA controls calcium homeostasis and exerts its anticancer effects. However, there could be alternative pathways for ion exchange. In addition, DHA suppressed the expression of ATP6V0B and ATP6V1F in the present study, suggesting that it may prevent the synthesis of additional ATP synthases. The present study demonstrated the regulatory role of CANX in liver cancer cell progression, especially its effects on mitochondrial function and energy metabolism. In addition, the potential anticancer effects of DHA by inhibiting

CANX expression was also assessed. Based on the results of various functional experiments, the effects of the CANX overexpression group and the DHA group are significantly opposite, while the DHA group is similar to the CANX overexpression combined with the DHA group. It is hypothesized that DHA may directly or indirectly inhibit the function of CANX. Although overexpression of CANX can produce a pro-oncogenic effect, DHA can significantly inhibit this effect brought about by CANX. These results suggest that DHA can significantly block or inhibit the action of CANX pcDNA3.1, indicating that CANX is an effective target for DHA (41,42).

Nevertheless, the present study has certain limitations, for example it was not elucidated how CANX influences calcium homeostasis through downstream genes, and the lack of validation in animal models limited the comprehensive evaluation of the therapeutic effects of DHA. Future studies should establish mouse xenograft models to evaluate the antitumor activity of DHA and enhance the understanding of its mechanisms.

In summary, CANX may be a crucial factor in the progression, diagnosis, treatment and prognostic evaluation of liver cancer. Its impact on the survival and metastasis of liver cancer cells is mediated through mitochondrial function and energy metabolism and the findings of the present study emphasize the anticancer role of DHA by inhibiting CANX and downregulating ATP6V0B and ATP6V1F expression.

Acknowledgements

Not applicable.

Funding

The present work was supported by the High-level Talents Project of Hainan Natural Science Foundation of 2022 (grant no. 822RC830) and the Hainan Health Industry Scientific Research Project of 2021 (grant no. 21A200072).

Availability of data and materials

The data generated in the present study may be requested from the corresponding author.

Authors' contributions

JC, QY, XL, WL and LG contributed to the study conception and design. Material preparation, data collection and analysis were performed by JC and QY. The first draft of the manuscript was written by JC and XL. Data analysis, writing and reviewing were performed by WL and LG. JC and LG confirm the authenticity of all the raw data. All authors commented on previous versions of the manuscript. All authors have read and approved the final manuscript.

Ethics approval and consent to participate

Not applicable.

Patient consent for publication

Not applicable.

Competing interests

The authors declare that they have no competing interests.

References

1. Lu LC, Hsu CH, Hsu C and Cheng AL: Tumor heterogeneity in hepatocellular carcinoma: Facing the challenges. Liver Cancer 5: 128-138, 2016.
2. Kobayashi M, Nagashio R, Jiang SX, Saito K, Tsuchiya B, Ryuge S, Katono K, Nakashima H, Fukuda E, Goshima N, *et al*: Calnexin is a novel sero-diagnostic marker for lung cancer. Lung Cancer 90: 342-345, 2015.
3. Ros M, Nguyen AT, Chia J, Le Tran S, Le Guezennec X, Mcdowall R, Vakhrushev S, Clausen H, Humphries MJ, Saltel F and Bard FA: ER-resident oxidoreductases are glycosylated and trafficked to the cell surface to promote matrix degradation by tumour cells. Nat Cell Biol 22: 1371-1381, 2020.
4. Garbincius JF and Elrod JW: Mitochondrial calcium exchange in physiology and disease. Physiol Rev 102: 893-992, 2022.
5. Wang LT, Lin MH, Liu KY, Chiou SS, Wang SN, Chai CY, Tseng LW, Chiou HC, Wang HC, Yokoyama KK, *et al*: WLS/wntless is essential in controlling dendritic cell homeostasis via a WNT signaling-independent mechanism. Autophagy 17: 4202-4217, 2021.
6. Zheng J, Yang T, Gao S, Cheng M, Shao Y, Xi Y, Guo L, Zhang D, Gao W, Zhang G, *et al*: miR-148a-3p silences the CANX/MHC-I pathway and impairs CD8(+) T cell-mediated immune attack in colorectal cancer. FASEB J 35: e21776, 2021.
7. Lam STT and Lim CJ: Cancer biology of the endoplasmic reticulum lectin chaperones calreticulin, calnexin and PDIA3/ERp57. Prog Mol Subcell Biol 59: 181-196, 2021.
8. Marshansky V, Rubinstein JL and Grüber G: Eukaryotic V-ATPase: Novel structural findings and functional insights. Biochim Biophys Acta 1837: 857-879, 2014.
9. Li X, Li H, Yang C, Liu L, Deng S and Li M: Comprehensive analysis of ATP6V1s family members in renal clear cell carcinoma with prognostic values. Front Oncol 10: 567970, 2020.
10. Hu X, Li D, Zhu H, Yu T, Xiong X and Xu X: ATP6V1F is a novel prognostic biomarker and potential immunotherapy target for hepatocellular carcinoma. BMC Med Genomics 16: 188, 2023.
11. Chen Y, Teng L, Liu W, Cao Y, Ding D, Wang W, Chen H, Li C and An R: Identification of biological targets of therapeutic intervention for clear cell renal cell carcinoma based on bioinformatics approach. Cancer Cell Int 16: 16, 2016.
12. Shen S, Du M, Liu Q, Gao P, Wang J, Liu S and Gu L: Development of GLUT1-targeting alkyl glucoside-modified dihydroartemisinin liposomes for cancer therapy. Nanoscale 12: 21901-21912, 2020.
13. Chang J, Xin C, Wang Y and Wang Y: Dihydroartemisinin inhibits liver cancer cell migration and invasion by reducing ATP synthase production through CaMKK2/NCLX. Oncol Lett 26: 540, 2023.
14. Luo Y, Ma J and Lu W: The significance of mitochondrial dysfunction in cancer. Int J Mol Sci 21: 5598, 2020.
15. Peoples JN, Saraf A, Ghazal N, Pham TT and Kwong JQ: Mitochondrial dysfunction and oxidative stress in heart disease. Exp Mol Med 51: 1-13, 2019.
16. Kang SW, Lee S and Lee EK: ROS and energy metabolism in cancer cells: Alliance for fast growth. Arch Pharm Res 38: 338-345, 2015.
17. Im H, Baek HJ, Yang E, Kim K, Oh SK, Lee JS, Kim H and Lee JM: ROS inhibits RORα degradation by decreasing its arginine methylation in liver cancer. Cancer Sci 114: 187-200, 2023.
18. Brown D, Paunescu TG, Breton S and Marshansky V: Regulation of the V-ATPase in kidney epithelial cells: Dual role in acid-base homeostasis and vesicle trafficking. J Exp Biol 212: 1762-1772, 2009.
19. Molinari M, Eriksson KK, Calanca V, Galli C, Cresswell P, Michalak M and Helenius A: Contrasting functions of calreticulin and calnexin in glycoprotein folding and ER quality control. Mol Cell 13: 125-135, 2004.
20. Kozlov G and Gehring K: Calnexin cycle - structural features of the ER chaperone system. FEBS J 287: 4322-4340, 2020.
21. Lüningschrör P, Andreska T, Veh A, Wolf D, Giridhar NJ, Moradi M, Denzel A and Sendtner M: Calnexin controls TrkB cell surface transport and ER-phagy in mouse cerebral cortex development. Dev Cell 58: 1733-1747.e6, 2023.

22. Yi YC, Liang R, Chen XY, Fan HN, Chen M, Zhang J and Zhu JS: Dihydroartemisinin suppresses the tumorigenesis and cycle progression of colorectal cancer by targeting CDK1/CCNB1/PLK1 signaling. Front Oncol 11: 768879, 2021.
23. Lim S, Ha Y, Lee B, Shin J and Rhim T: Calnexin as a dual-role biomarker: Antibody-based diagnosis and therapeutic targeting in lung cancer. BMB Rep 57: 155-160, 2024.
24. Luo L, Li P, Xie Q, Wu Y, Qin F, Liao D, Zeng K and Wang K: n6-methyladenosine-modified circular RNA family with sequence similarity 126, member A affects cholesterol synthesis and malignant progression of prostate cancer cells by targeting microRNA-505-3p to mediate calnexin. J Cancer 15: 966-980, 2024.
25. Ruiz C, Alborelli I, Manzo M, Calgua B, Keller EB, Vuaroqueaux V, Quagliata L, Rentsch CA, Spagnoli GC, Diener PA, *et al*: Critical evaluation of transcripts and long noncoding RNA expression levels in prostate cancer following radical prostatectomy. Pathobiology 90: 400-408, 2023.
26. Pavlakis E, Neumann M, Merle N, Wieboldt R, Wanzel M, Ponath V, Pogge Von Strandmann E, Elmshäuser S and Stiewe T: Mutant p53-ENTPD5 control of the calnexin/calreticulin cycle: A druggable target for inhibiting integrin-α5-driven metastasis. J Exp Clin Cancer Res 42: 203, 2023.
27. Cheng J, Zhang G, Deng T, Liu Z, Zhang M, Zhang P, Adeshakin FO, Niu X, Yan D, Wan X and Yu G: CD317 maintains proteostasis and cell survival in response to proteasome inhibitors by targeting calnexin for RACK1-mediated autophagic degradation. Cell Death Dis 14: 333, 2023.
28. Ryan D, Carberry S, Murphy ÁC, Lindner AU, Fay J, Hector S, Mccawley N, Bacon O, Concannon CG, Kay EW, *et al*: Calnexin, an ER stress-induced protein, is a prognostic marker and potential therapeutic target in colorectal cancer. J Transl Med 14: 196, 2016.
29. Okayama A, Miyagi Y, Oshita F, Nishi M, Nakamura Y, Nagashima Y, Akimoto K, Ryo A and Hirano H: Proteomic analysis of proteins related to prognosis of lung adenocarcinoma. J Proteome Res 13: 4686-4694, 2014.
30. Stahon KE, Bastian C, Griffith S, Kidd GJ, Brunet S and Baltan S: Age-related changes in axonal and mitochondrial ultrastructure and function in white matter. J Neurosci 36: 9990-10001, 2016.
31. Gutiérrez T and Simmen T: Endoplasmic reticulum chaperones tweak the mitochondrial calcium rheostat to control metabolism and cell death. Cell Calcium 70: 64-75, 2018.
32. Du C, Guo X, Qiu X, Jiang W, Wang X, An H, Wang J, Luo Y, Du Q, Wang R, *et al*: Self-reinforced bimetallic mito-jammer for Ca(2+) overload-mediated cascade mitochondrial damage for cancer cuproptosis sensitization. Adv Sci (Weinh) 11: e2306031, 2024.
33. Kim S, Ramalho TR and Haynes CM: Regulation of proteostasis and innate immunity via mitochondria-nuclear communication. J Cell Biol 223: e202310005, 2024.
34. Radif Y, Ndiaye H, Kalantzi V, Jacobs R, Hall A, Minogue S and Waugh MG: The endogenous subcellular localisations of the long chain fatty acid-activating enzymes ACSL3 and ACSL4 in sarcoma and breast cancer cells. Mol Cell Biochem 448: 275-286, 2018.
35. Haugen ØP, Khuu C, Weidemann HM, Utheim TP and Bergersen LH: Transcriptomic and functional studies reveal miR-431-5p as a tumour suppressor in pancreatic ductal adenocarcinoma cells. Gene 822: 146346, 2022.
36. Chen F, Kang R, Liu J and Tang D: The V-ATPases in cancer and cell death. Cancer Gene Ther 29: 1529-1541, 2022.
37. Huang P, Xia L, Guo Q, Huang C, Wang Z, Huang Y, Qin S, Leng W and Li D: Genome-wide association studies identify miRNA-194 as a prognostic biomarker for gastrointestinal cancer by targeting ATP6V1F, PPP1R14B, BTF3L4 and SLC7A5. Front Oncol 12: 1025594, 2022.
38. Singh J, Meena A and Luqman S: New frontiers in the design and discovery of therapeutics that target calcium ion signaling: A novel approach in the fight against cancer. Expert Opin Drug Discov 18: 1379-1392, 2023.
39. Kannurpatti SS: Mitochondrial calcium homeostasis: Implications for neurovascular and neurometabolic coupling. J Cereb Blood Flow Metab 37: 381-395, 2017.
40. De Marchi U, Santo-Domingo J, Castelbou C, Sekler I, Wiederkehr A and Demaurex N: NCLX protein, but not LETM1, mediates mitochondrial Ca2+ extrusion, thereby limiting Ca2+-induced NAD(P)H production and modulating matrix redox state. J Biol Chem 289: 20377-20385, 2014.
41. Ma Y, Zhang P, Zhang Q, Wang X, Miao Q, Lyu X, Cui B and Ma H: Dihydroartemisinin suppresses proliferation, migration, the Wnt/β-catenin pathway and EMT via TNKS in gastric cancer. Oncol Lett 22: 688, 2021.
42. Wang X, Guo P, Tian J, Li J, Yan N, Zhao X and Ma Y: LncRNA GAS5 participates in childhood pneumonia by inhibiting cell apoptosis and promoting SHIP-1 expression via downregulating miR-155. BMC Pulm Med 21: 362, 2021.